

M.A. Korzhuev, T.E. Svechnikova



M.A. Korzhuev

A.A. Baikov Institute of Metallurgy and Material
Science of RAS, 49, Leninskiy Ave.,
Moscow, 119991, Russia



T.E. Svechnikova

**THERMODYNAMIC RESTRICTIONS FOR
THE NET POWER OF AUTOMOTIVE
THERMOELECTRIC GENERATORS AND
PROSPECTS OF THEIR USE IN TRANSPORT**

Experimental characteristics of automotive thermoelectric generators (ATEGs) placed on exhaust pipe (EP) are analyzed. It is shown that low net powers $W_e = 0.2 - 0.6$ kW and inefficient automotive waste heat recovery (WHR) using ATEG (total gain in car power $\Delta W \sim 0$) are related to the difficulties of heat exchange on the “exhaust gas (EG)/ ATEG” boundary. As a result, the specific power of ATEG also appears to be low $\tilde{W}^{ATEG} = W_e/m^{ATEG} \sim 20 - 30$ W/kg (here, m^{ATEG} is ATEG mass). Low values of W_e and \tilde{W}^{ATEG} are explained in the framework of A.S. Okhotin theory taking into account high thermal resistances of ATEG heat exchangers. It is shown that using A.F. Ioffe theory that does not take into account thermal resistances of heat exchangers, yields overestimated values of W_e , ΔW , \tilde{W}^{ATEG} and efficiency η^{ATEG} , and also the incorrect prediction of optimum energy gap E_g^{opt} of the leg materials. It is shown that the prospects of using high-power ATEGs in cars are essentially limited today. The ways for improvement of ATEG characteristics are discussed.

Key words: thermoelectricity, cars, waste heat recovery.

Introduction

At the present time, the world car park has exceeded ~ 1 billion units. As a result, cars have become the main pollutants of the Earth atmosphere by exhaust gases (EG) and waste heat [1]. Internal combustion engines (ICE) of modern cars have rather high efficiency $\eta^{ICE} \sim 0.4$ [2]. However, the major part of burning fuel power Q_0 and part of the net power of internal combustion engine $W^{ICE} = \eta^{ICE} Q_0$ are irretrievably lost through the exhaust pipe (EP) ($Q_0^{EP} \sim 0.3Q_0$), cooling system (CS) ($Q_0^{CS} \sim 0.3Q_0$), transmission and auxiliary mechanisms of a car (L) ($Q_0^L \sim 0.2Q_0$) (Fig. 1 a). As a result, to overcome the motion resistance force of a car F_R , power consumption does not exceed $W_T^{AUTO} \sim \frac{1}{2}W^{ICE} \sim 0.2 Q_0$ [3, 4]. Hence, a need for waste heat recovery and fuel saving in cars [1, 4-6] is created. For these purposes, since the mid XX century in various countries automotive thermoelectric generators (ATEGs) have been developed, that are usually placed on the exhaust pipe of a car (Fig. 1 b) [3-12]. In this case, part of exhaust heat ($Q_0^{ATEG} < Q_0^{EP}$) is taken away to ATEG input and converted into net electric power $W_e = \eta^{ATEG} Q_0^{ATEG}$ via the Seebeck effect. (Here η^{ATEG} and Q_0^{ATEG} are the efficiency and thermal flux power at ATEG input) (Fig. 1 b) [1, 2]. As a result, on condition of $V_0 = \text{const}$, car power will increase by the value $\Delta W = W_e$, and the relative fuel consumption will be reduced accordingly $\delta A = \Delta A/A \sim -\Delta W/0.2 Q_0 < 0$ (Here A is the initial fuel consumption by a car, ΔA is its change after installation of ATEG, V_0 is car speed) [4, 13].

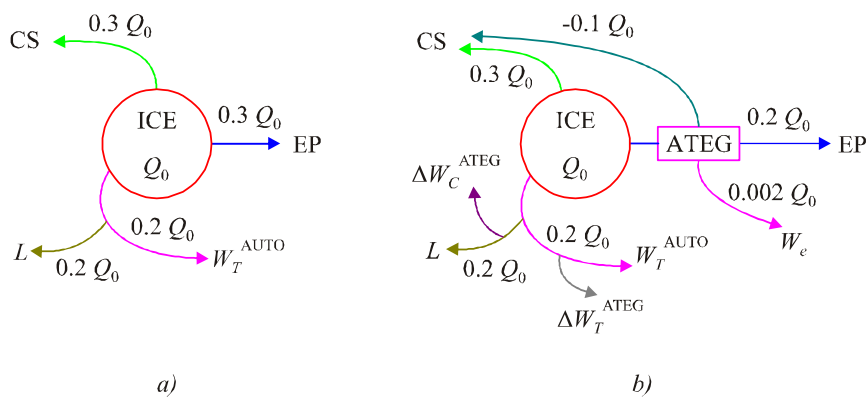


Fig. 1. Heat and energy fluxes in a car before (a) and after (b) ATEG installation on exhaust pipe.

Here, Q_0 and W_T^{AUTO} – power of burning fuel and its share spent for car motion;
 L – losses in car mechanisms; ΔW_T^{ATEG} and ΔW_C^{ATEG} – losses due to ATEG transportation and cooling
 ($\eta^{ATEG} = 0.02$; $W_e = 0.2 \text{ kW}$; $\Delta W_T^{ATEG} = 0.1 \text{ kW}$; $\Delta W_C^{ATEG} = 0.2 \text{ kW}$).

However, in practice the ratio $\Delta W = W_e$ in a car is never fulfilled because ATEG needs part of ICE power $\Delta W^{ICE} = \Delta W_T^{ATEG} + \Delta W_C^{ATEG}$ for its transportation ($\Delta W_T^{ATEG} > 0$) and forced cooling of the cold junctions ($\Delta W_C^{ATEG} \geq 0$) (Fig. 1 b) [13-15]. In this case, the waste heat recovery power of a car is reduced accordingly to

$$\Delta W = W_e - \Delta W_T^{ATEG} - \Delta W_C^{ATEG} \quad (1)$$

and even becomes negative, if service expenses ΔW_T^{ATEG} and ΔW_C^{ATEG} are significant [13-15]. Thus, in practice, there are two main modes of ATEG operation in a car: 1) real waste heat recovery with fuel economy ($0 < \Delta W < W_e$, $\delta A < 0$), and 2) simple energy generation, when no real waste heat recovery takes place, and total fuel consumption and greenhouse gas emission by cars is increased ($\Delta W < 0 < W_e$, $\delta A > 0$) [13-18].

The purpose of this study was to investigate the current state of ATEG problem. The experimental characteristics of serial ATEG prototypes developed recently for motorcycles, cars and trucks [1-5, 7] are analyzed. It is shown that in all the cases the performance characteristics of ATEG are significantly lower than expected by developers, owing to which the majority of ATEGs work in low-efficient simple energy generation mode [3, 6, 13]. Low efficiency of modern ATEGs is attributable in the paper to thermodynamic limitations of their specific power $\hat{W}^{ATEG} = W_e/m^{ATEG} < 20 - 30 \text{ W/kg}$ (here m^{ATEG} – ATEG mass) in "CAR + ATEG" system. Low values of \hat{W}^{ATEG} are explained in the paper through use of A.S. Okhotin theory [20], taking into account high parasitic thermal resistances of ATEG heat exchangers (R_{HE}^{ATEG}) on the "exhaust gas/ATEG" boundary. It is shown that because of consistently high R_{HE}^{ATEG} the prospects of using high-power ATEGs in cars are considerably limited today. Various ways for enhancement of ATEG performance are discussed, of which improvement of their heat exchangers seems to be most important.

1. "CAR-ATEG" system

Placing of ATEG in a car forms a complex thermodynamic system "CAR-ATEG" containing two dissimilar heat engines (ICE and ATEG) [13-15]. ATEG installation increases the overall mass of a car $m^{AUTO+ATEG} = m^{AUTO} + m^{ATEG}$ and its front dimensions $\Delta S^{AUTO+ATEG} \approx \Delta S^{AUTO} + \Delta S^{ATEG}$, resulting in increased motion resistance force $F_R \rightarrow F_R + \Delta F_R$ (Here m^{AUTO} is mass of a car, and ΔS^{AUTO} and ΔS^{ATEG} are front dimensions of a car and ATEG, respectively ($a \rightarrow b$, Figure 2) [3]. Moreover, with

increase in $W_e > 0$, conflict between heat engines (ICE and ATEG) is developed in "CAR-ATEG" system. The conflict is due to competition of heat engines for sources and sinks of heat in the system [14]. Development of the conflict between heat engines in "CAR-ATEG" system reduces the efficiency of the ICE and restricts increase in W_e and ΔW of ATEG [13-18]. The influence of all factors discussed above on the experimental characteristics of ATEG is considered below.

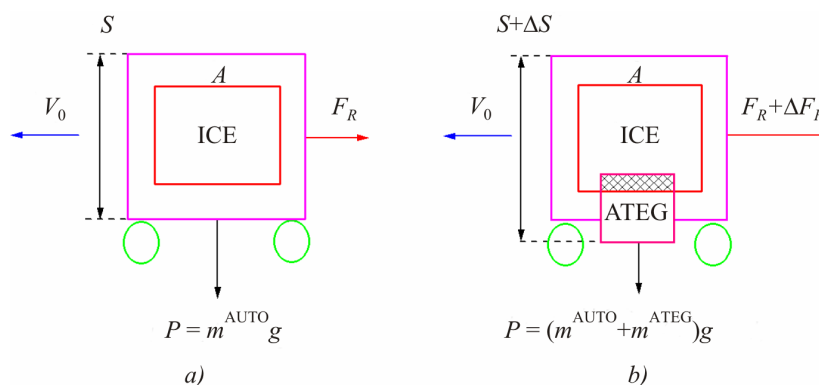


Fig. 2. Changes in mass m , weight P , front dimensions ΔS , motion resistance force ΔF_R and development of a conflict between heat engines (internal combustion engine and ATEG) (shaded area) with ATEG installation on a car (A) ($a \rightarrow b$).

1.1. Experimental characteristics of ATEG

Table 1 shows the experimental characteristics of serial ATEG prototypes designed for motorcycles, cars, pickups and trucks [1, 2-7]. According to [1, 2-7], we have calculated the specific power of vehicles $\hat{W}^{\text{AUTO}} = W^{\text{AUTO}}/m^{\text{AUTO}}$ and the specific power of installed ATEG $\hat{W}^{\text{ATEG}} = W_e/m^{\text{ATEG}}$, waste heat recovery power ΔW and a change in fuel consumption δA with ATEG operated at full capacity (Table 1). In the calculations we used the ratio (1) assuming for simplicity $\Delta W_C = 0$; $\Delta W_T^{\text{ATEG}} = \Delta W_{T1}^{\text{ATEG}} + \Delta W_{T2}^{\text{ATEG}}$ (Here $\Delta W_{T1}^{\text{ATEG}} = 0.1 W^{\text{ICE}} \cdot m^*$ and $\Delta W_{T2}^{\text{ATEG}} = 0.1 W^{\text{ICE}} S^*$ are additional expenditures of engine power to overcome rolling friction and air resistance when driving, $m^* = m^{\text{ATEG}}/m^{\text{AUTO}}$ and $S^* = \Delta S^{\text{ATEG}}/S^{\text{AUTO}}$ are the mass-factor and form-factor of ATEG in a car). Table 1 shows that the operating efficiency of modern ATEGs (Table 1) is generally low.¹ Maximum W_e values of ATEG did not exceed $\sim 1/3 - 2/3$ of the calculated values needed to power the vehicles. In so doing, all ATEGs (Table 1) were operated mainly in a low-efficiency simple energy generation mode (SEG) ($\Delta W < 0$) (motorcycles, cars), or in the mode of real waste heat recovery which is close to simple energy generation mode (pickups, trucks). A change in SEG \rightarrow WHR mode (Table 1) was due to a decrease in mass-factor m^* and form-factor S^* of ATEG in motorcycle \rightarrow truck series.

As a result, in practice, the real waste heat recovery was possible only for trucks ($m^{\text{AUTO}} > 6$ t; $\Delta W > 0$, $\delta A < 0$), but not for cars, pickups ($m^{\text{AUTO}} = 2 - 5$ t; $\Delta W \sim 0$, $\delta A \sim 0$) and motorcycles ($m^{\text{AUTO}} \ll 1$ t; $\Delta W < 0$, $\delta A > 0$). From Table 1 it is also evident that at $m^* = \text{const}$ the waste heat recovery power ΔW can be increased by reducing the form-factor of ATEG ($S^* \rightarrow 0$).² In this case the value of ΔW will be only limited by two main factors – W_e and m^{ATEG} determining specific power \hat{W}^{ATEG} . According to our calculations, the specific powers of ATEG for all vehicles proved to be low $\hat{W}^{\text{ATEG}} < 20 - 30$ W/kg, and never exceeded even the specific power of internal combustion engine spent on vehicle motion $\hat{W}_T^{\text{AUTO}} = \frac{1}{2} \hat{W}^{\text{ICE}} \sim 15 - 26$ W/kg (Table 1) [4, 13]. As a result, for motorcycles, cars

¹ Characteristics of ATEG (Table 1) were obtained when driving on the highway at a limit speed $V_0 \sim 110 - 150$ km/h. When driving in the city ($V_0 \sim 30 - 60$ km/h), they will be reduced by a factor of 3 to 6 again.

² It can be done due to the use of air cowls and flush mounting of ATEG [3, 9].

and pickups we have $\dot{W}_T^{\text{AUTO}} > \dot{W}_e$, that is, the gain in the total power of a car due to net power W_e of ATEG does not compensate ICE service costs even for ATEG transportation (Table 1). On the contrary, for trucks we get $W_e > W_T$, which is related to their relatively low specific power expenditures on motion ($\dot{W}^{\text{AUTO}} < \dot{W}^{\text{ATEG}}$) (Table 1). The issue of low specific power \dot{W}^{ATEG} calls for special discussion.

Table 1

Characteristics of serial ATEG prototypes designed for various vehicles [1, 2-7]

№	Characteristics	Motorcycle ^a	Car ^b	Pickup ^c	Truck ^d
1. Vehicle	Engine displacement V , l and type	0.4 G	3.4 D	5.3 G	14 D
	Internal combustion engine power, W^{ICE} , kW	7.4	125	146	162
	Mass, m^{AUTO} , kg	150	1545	2770	10000
	Specific power \dot{W}^{AUTO} , W/kg	49	81	53	16.2
	Specific power of motion, $\dot{W}_T^{\text{AUTO}} = 1/2 \dot{W}^{\text{ICE}}$, W/kg	24	40	26	8
	Front size S^{AUTO} , m ²	0.7	2.5	4	5
2. ATEG	Achieved maximum power W_e , W	10	200	300* 600**	400*** 1000****
	Necessary power, W_e^* , W	100 – 200	~ 600	~ 1000	> 1000
	Material of ATEG legs	Fe_2VAl	$(Bi, Sb)_2Te_3$	$PbTe$	$(Bi, Sb)_2Te_3$
	Mass, m^{ATEG} , kg	~ 3	13	39.1	13
	Specific power \dot{W}^{ATEG} , W/kg	3.3	15	7.7* 15.4**	30,8*** 76.9****
	Dimensions, ΔS^{ATEG} , cm ²	100	220	590	412
	Mass-factor, m^*	0.02	0.008	0.014	0.001
	Form-factor, S^*	0.014	0.009	0.015	0.008
3. Power losses	Losses due to mass-factor, W_{T1}^{ATEG} , W	20	143	279	29
	Losses due to form-factor, W_{T2}^{ATEG} , W	14	149	292	180
	Total power gain, $\Delta W = (W_e - W_{T1}^{\text{ATEG}} - W_{T2}^{\text{ATEG}})$, W	-24	-92	-271* 29**	191*** 791****
	Change in fuel consumption, $\delta A = \Delta W / (0.2 Q_0)$, %	0.65	0.15	0.37* -0.04**	-0.24*** -0.97****

^{a)} Suzuki ¹⁰; ^{b)} BMW531 ^{5, 6}; ^{c)} GM Sierra 1500 ³; ^{d)} Engine NTC-350 ³; * – traffic in the city ($V_0 \sim 60$ km/h); ** – traffic on the highway ($V_0 \sim 110 - 150$ km/h)³; *** – received; **** – expected. G – gasoline, D – diesel.

1.2. Low specific power of ATEG

Table 2 shows a comparison of the specific power \dot{W}^{ATEG} to the specific power of thermoelectric generators (TEG) of other types (\dot{W}^{TEG}) using solid or liquid heat carriers [19, 21-23].

According to Table 2, using the same thermoelectric materials (TEM) we have $\hat{W}^{\text{TEG}}/\hat{W}^{\text{ATEG}} \geq 10 - 20$. Accordingly, provided $W_e = \text{const}$, the masses of ATEG will exceed considerably the masses of other types of TEG ($m^{\text{ATEG}}/m^{\text{TEG}} \sim 10 - 30$ and more) (Table 2).

Table 2

Comparison of specific power \hat{W}^{ATEG} to that of thermoelectric generators of other types \hat{W}^{TEG} using liquid or solid heat carriers

Material of legs	Density d , g/cm ³	Specific power \hat{W} , kW/kg		$\hat{W}^{\text{TEG}}/\hat{W}^{\text{ATEG}}$ ratio
		ATEG	Other TEGs	
<i>Bi-Sb-Te-Se</i>	6.5 – 7.8	0.015 [3]	0.17 – 0.3 [21] ~ 0.2 [4]	11 – 20
<i>PbTe</i>	8.16	0.008 – 0.015 [3]	0.2 – 0.25 [4, 21]	13 – 31
<i>Si-Ge</i>	2.5 – 2.9	0.003 [3, 8]	≤ 1.2 [21]	400
<i>Mg₂Si_{0.4}Sn_{0.6}</i>	~ 2.9	~ 0.07 – 0.1 [8, 23]	~ 0.8 – 1 [23]	8 – 14

As is known, the mass of legs m_L necessary for production of assigned net power of TEG W_e is given by the expression

$$m_L = Vd = 2W_e l^2 d / (A\Delta T^2), \quad (2)$$

where V and d are the volume and density of thermoelectric material, l is the height of legs; $A = Z\kappa = \alpha^2\sigma$ is power factor; α , σ and κ are the Seebeck coefficient, specific electric and heat conductivity of legs, and ΔT is operating temperature difference on thermocouple legs [22]. From Eq. (2) it follows that for the same TEM (A , $d = \text{const}$) the ratio $\hat{W}^{\text{TEG}}/\hat{W}^{\text{ATEG}} \sim 10 - 30$ (Table 2) can be explained by increased ATEG height l and reduced operating temperature differences ΔT on their legs. Comparison of the TEG and ATEG design features has confirmed this assumption. Indeed, the height of ATEG legs reaches $l^{\text{ATEG}} \sim 5, 7.5$ and 10 mm [3, 4, 7, 22], whereas in other types of TEG it is significantly lower (usually $l^{\text{TEG}} = 1 - 3$ mm) [21, 23]. In the same way, the operating temperature differences on ATEG legs are much lower $\Delta T^{\text{ATEG}} \sim \frac{1}{2}\Delta T_0$ [9, 24] compared to other types of TEG, where usually $\Delta T^{\text{TEG}} \sim \Delta T_0$. (Here ΔT_0 is the available temperature difference provided by the source of heat) [21, 23]. As a result, other things being equal, we have $W_e^{\text{TEG}}/W_e^{\text{ATEG}} \sim 2$, $m^{\text{ATEG}}/m^{\text{TEG}} \sim 2$, which yields $\hat{W}^{\text{TEG}}/\hat{W}^{\text{ATEG}} \sim 10 - 20$ in accordance with Table 2. Low \hat{W}^{ATEG} values are attributable below to difficulties of heat exchange in "CAR+ATEG" system [2, 13-15].

2. ATEG calculations

2.1. Heat exchange in "CAR+ATEG" system

Unlike the internal combustion engine, ATEG is the "external" combustion engine, so it needs two additional heat exchangers connected to heat sources and sinks in a car [2, 15]. Heat removal from ATEG is generally provided by "standard" or additional autonomous cooling system with water or air cooling [3-6].³ As sources of heat for ATEG, apart from the exhaust pipe, we will also consider internal combustion engine and cooling system having additional reserves for waste heat recovery of cars (Fig. 1). Heat in a car is transferred by hot gases from the internal combustion engine to exhaust pipe, and also by a coolant (water and/or air) through cooling system to atmosphere. Heat in ATEG is

³ The use of standard car cooling system is considered to be optimum [3, 4].

transferred by electrons and phonons due to thermal conductivity of legs and the Peltier effect (in energy generation mode) [2, 17]. In so doing, the mechanisms of heat transfer in ATEG appear less efficient than combined heat and mass transfer in the pipes [13-15]. As a result, thermal resistance of ATEG (R_T^{ATEG}) essentially exceeds thermal resistances of internal combustion engine, exhaust pipe and cooling system ($R_T^{\text{ICE, EP, CS}}$) which determines the difficulties of heat exchange in the system [13, 14]. Besides, as mass transfer in ATEG legs is impossible⁴, for heat removal to ATEG in a car one can use only parallel connection of ATEG to the pipes [13, 16]. In this case it is possible to take away to ATEG not the entire heat flux in a pipe ($Q_0^{\text{ICE, EP, CS}}$), but only its small part $Q_0^{\text{ATEG}} \sim Q_0^{\text{ICE, EP, CS}} \cdot R_T^{\text{ICE, EP, CS}} / (R_T^{\text{ATEG}} + R_T^{\text{ICE, EP, CS}}) \ll Q_0$, inversely proportional to R_T^{ATEG} .

The scheme of parallel connection of ATEG to exhaust pipe is shown in Fig. 3. From Fig. 3 it is seen that process of heat removal from exhaust gas to ATEG (arrow) is interfered by motionless gas and coke layers with a low heat conductivity adsorbed on the "exhaust gas/exhaust pipe" heat exchange boundary (2, 4) [2, 23, 26]. A layer of adsorbed gas (of thickness $d \sim 1 - 2$ microns) is constantly present on the inside of exhaust pipe at any velocities of exhaust gas motion in it (V^{EP}) (2, Fig. 3) [2]. Thus, coke layers (4, Fig. 3) can achieve thickness $c \sim 1$ mm and more in the "cold" parts of exhaust pipe [13, 16].

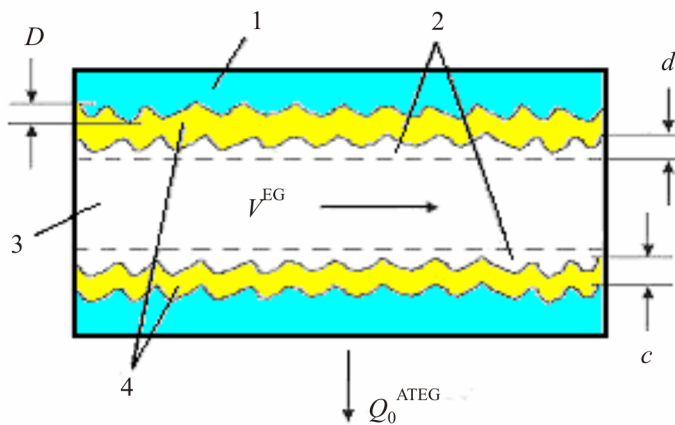


Fig. 3. Parallel connection of ATEG to exhaust pipe. 1 – exhaust pipe case; 2 – adsorbed gas layer; 3 – exhaust gas; 4 – carbon deposit; d, c – gas and carbon deposit layers; V^{EG} – exhaust gas velocity; D – roughness of exhaust pipe internal surface, Q_0^{ATEG} – input heat flux of ATEG.

Owing to high thermal resistances of the adsorbed layers (2, 4, Fig. 3), the thermal resistances of ATEG essentially increase. Thus, input heat fluxes Q_0^{ATEG} and the operating temperature difference on ATEG legs decrease accordingly $\Delta T \sim \Delta T_0 \cdot R_T^{\text{ATEG}} / (R_{\text{HE}}^T + R_T^{\text{ATEG}})$ [11, 13, and 24]. We have taken into account the above peculiarities of heat exchange in "CAR + ATEG" system in deciding on ATEG thermal model [13].

2.2. ATEG thermal model

ATEG thermal model used in the work is shown in Fig. 4 [13]. The model (Fig. 4) takes into account thermal resistances of exhaust pipe $R_{\text{EP}}^T = R_0^T + R_1^T$ (here R_0^T and R_1^T are the beginning and the remaining portion of exhaust pipe), thermocouple legs R_3^T , and also "hot" and "cold" heat exchangers R_2^T and R_4^T of ATEG ($R_{\text{TO}}^T = R_2^T + R_4^T$). The formulae for calculation of ATEG parameters for the model (Fig. 4) corresponding to maximum power (I), or maximum efficiency (II) modes are presented in Table 3. Two boundary conditions were used: 1) constant temperature of junctions ($T_h = \text{const}, T_c = \text{const}$) (The theory of A.F. Ioffe) [19] and 2) constant temperature of heat-carriers ($T_h' = \text{const}, T_c' = \text{const}$) (The theory of A.S. Okhotin) [20].

⁴ Exception is provided by "permeable" thermoelements [25].

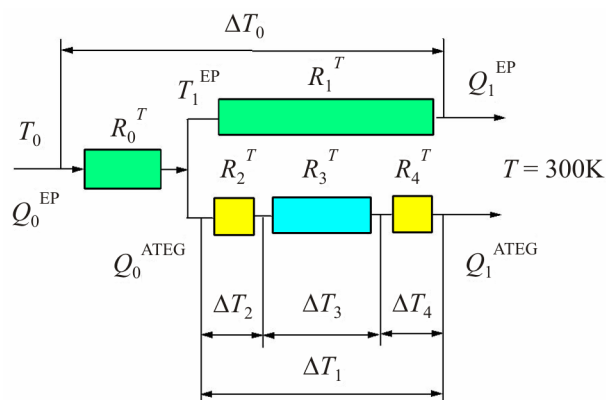


Fig. 4. Thermal model of parallel connection of ATEG to exhaust pipe and the respective temperature differences ΔT_i (ATEG idling mode). Thermal resistances of segments: R_0^T – exhaust pipe beginning; R_1^T – exhaust pipe remainder; R_3^T – thermocouple legs; R_2^T and R_4^T – “hot” and “cold” heat exchangers of ATEG [13].

Table 3

Optimum parameters of thermoelectric generators operated in the modes of maximum power (I) and maximum efficiency (II) under various boundary conditions (the shaded area is for ratios suitable for calculations of ATEG) *

Mode	Parameters	Boundary conditions	
		Fixed temperature of junctions: $T_h = \text{const}$, $T_c = \text{const}$ [11]	Fixed temperature of heat carriers: $T_h' = \text{const}$, $T_c' = \text{const}$ [12]
I. Maximum power	Relative electric load, $M = R/r$	1	$A^* = M_0$
	Power, W_e^{\max}	$E_{ID}^2/(4r) = W\Delta T^2/4$	$E_{ID}^2/(4A^*r) = W\Delta T^2/4A^*$
	Temperature difference on the legs, ΔT	$(T_h - T_c)$	$(T_h' - T_c')(A^* + 1)/(4A^*)$
	Efficiency, $\eta (W_e^{\max})$	$\eta_c/(2 + 4/ZT_h - \eta_c/2)$	$\sim 0.22 \eta_c(M_0 - 1)/(M_0 + T_c'/T_h')$
	Optimum dimensionless height of legs, l_0	$\beta \sim 0.1$	$Bi = M_0$
II. Maximum efficiency	Relative electric load, $M = R/r$	M_0	M_0
	Temperature difference on the legs, ΔT	$(T_h - T_c)$	$(T_h' - T_c')$
	Power, $W_e (\eta_{\max})$	$M_0 E_{SC}^2/[r(1 + M_0)^2]$	0
	Efficiency, η_{\max}	$\eta_c(M_0 - 1)/(M_0 + T_c/T_h)$	$\eta_c(M_0 - 1)/(M_0 + T_c'/T_h')$
	Optimum height of legs, l_0	∞	∞

Here: $M = R/r$ is relative electric load of ATEG; R is electric resistance of load; $r = r_0(1 + \beta)$ is electric resistance of ATEG; r_0 is electric resistance of legs; $\beta = (r_j + r_c)/r_{sc}$ is factor of electric losses; r_j , r_c and r_{sc} are electric resistances of contacts, connecting plates and semiconductor material of legs, $M_0 = (1 + Z\bar{T})^{1/2}$; $Z = Z_0/(1 + \beta)$ and Z_0 is the thermoelectric figure of merit of TEG with and without account of electric losses; $T = 1/2(T_h + T_c)$ is the average temperature; $E_{ID, SC} = (\alpha_p - \alpha_n) \Delta T^{ID, SC}$ are termoEMF in idling and short circuit mode of thermocouples; $\eta_c = (T_h - T_c)/T_h$ is the Carnot factor; $A^* = (1 + Z\bar{T})/(1 + Bi)$ is the ATEG's constant; $R^T = (R_3 + R_4 + R_5)$ – the sum of thermal resistances of legs and heat spreaders; $Bi = R_{nm}^T / R_{mo}^T$ – the ratio of thermal resistances of semiconductor legs of ATEG and heat exchangers (integral Biot criterion of ATEG).

Comparison of Fig. 4 and Table 3 shows that the Ioffe theory [19] takes into account only the contribution of thermocouple legs (R_3^T) and their contact electric resistances (through parameter β) to overall thermal and electrical balance of ATEG ($R_3^T \neq 0, R_0^T = R_1^T = R_2^T = R_4^T = 0$, the integral Biot criterion of ATEG $Bi = R_3^T / (R_2^T + R_4^T) = \infty$) (Fig. 4). However, in real practice for all ATEGs we have $Bi \sim 1$ [13], so the Ioffe theory [19] is not the best approximation for ATEG [20]. It is shown below that the Okhotin theory [20] that takes into account the contribution of ATEG heat exchangers R_{TO}^T to thermal balance of the system ($R_2^T, R_3^T, R_4^T \neq 0, Bi \sim 1$, Fig. 4) is best suited for the calculations of ATEG.

2.3. The Ioffe and Okhotin theories

For the calculations of ATEG we employed a cylindrical layered model of length $L = 0.6$ m, with an internal diameter $D = 0.05$ m [13]. The optimal height of ATEG legs $l = 0.5$ cm (for Bi_2Te_3) was estimated from the condition $Bi = M_0$ (Table 3). In the calculations, the film thickness of the adsorbed gas on the surface of the heat exchange “exhaust gas/exhaust pipe” was assumed equal to the roughness of exhaust pipe ($d \sim D \approx 0.0001$ m) (2, Fig. 3). The contribution of coke layer (4, Fig. 3) to R_2 for simplicity was not taken into account [13]. Calculations were made using Ohm's and Kirchhoff's laws for electrical and thermal circuits of ATEG. [13]. In our calculations we employed the values $Q_0^{ICE, EP, CS} = Q_0; 0.3 Q_0; 0.3 Q_0; \Delta T_0^{ICE, EP, CS} \sim 1400; 650; 50$ K and $Q_0 = 100$ kW (gasoline engine $W^{ICE} \approx 54$ h.p.).

Figure 5 shows the results of calculation of the thermal resistances $R^T = \Delta T/Q$ (A) and available thermal heads ($Q\Delta T$) (B) for internal combustion engine (the area of combustion chamber), exhaust pipe and cooling system (the area from ICE water "jacket" to radiator) with water (4) and air cooling (5) of ATEG. From Figure 5 it follows that in all the cases the relation $R_T^{ATEG} \gg R_T^{ICE, EP, CS}$ is fulfilled, and in going from water cooling to air cooling, the thermal resistance R_T^{ATEG} further increased by a factor of ~ 2 ($4 \rightarrow 5$). Thus, below we will consider the case of ATEG water cooling only ($R_4^T = 0$).⁵

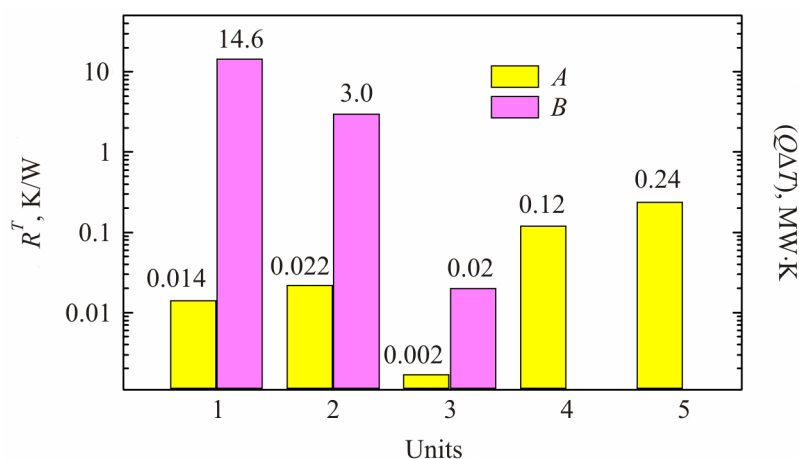


Fig. 5. Thermal resistances $R^T = \Delta T/Q$ (A) and available thermal heads ($Q\Delta T$) (B) for different car units. 1 – internal combustion engine; 2 – exhaust pipe; 3 – cooling system; 4 – 5 – standard size ATEG with Bi_2Te_3 legs ($l = 5$ mm). ATEG cooling: 4 – water; 5 – air (calculated according to model in Fig. 4, at $R_0 = 0$).

Figs. 6 – 8 show the dependences of the efficiency η^{ATEG} , as well as operating temperature difference on the legs ΔT and the optimum height of the legs l versus the ZT of the samples, calculated using the

⁵ If necessary, ATEG air cooling is used only in motorcycles [1, 7].

theories of Ioffe [19] and Okhotin [20] in maximum efficiency and maximum power modes (Table 3). According to our calculations, in maximum efficiency mode the values of η in the theories of Ioffe [19] and Okhotin [20] coincide (curve 1, Figure 6). However, when passing to the mode of maximum power (which is the operation mode of ATEG), these theories yield significantly different values of η_W . The Ioffe theory gives $\eta_W \sim 0.8 \cdot \eta$, and the Okhotin theory – $\eta_W \sim 0.22 \cdot \eta$ (curves 2 and 3, Figure 6).

In addition, in maximum power mode, the Okhotin theory [20] predicts the dependence of the temperature difference ΔT on ATEG legs on the ratio of its thermal and electrical characteristics (A^* and M). As a result, the expected values of W_e and the optimum height of the legs l are also found to depend on the thermal resistances of heat exchangers ($R_2^T, R_4^T \neq 0$) and the relative electrical load $M = R/r$ of ATEG (I, Table 3). This significant difference between the Ioffe [19] and Okhotin [20] theories (Fig. 6 – 8) is due to account in the theory [20] of the contribution of large parasitic thermal resistances of heat exchangers R_2^T and R_4^T (Fig. 4), which in the theory [19] are assumed equal to zero. This result can be explained by the known rule of H. Lenz (Figure 9), which is applicable to any source of energy operated in maximum power mode [27, 28]. Since any TEG is a thermal and electric engine simultaneously, Lenz's rule, generally speaking, should be applied to it twice, namely, first to the thermal, and then to the electric circuits [17].

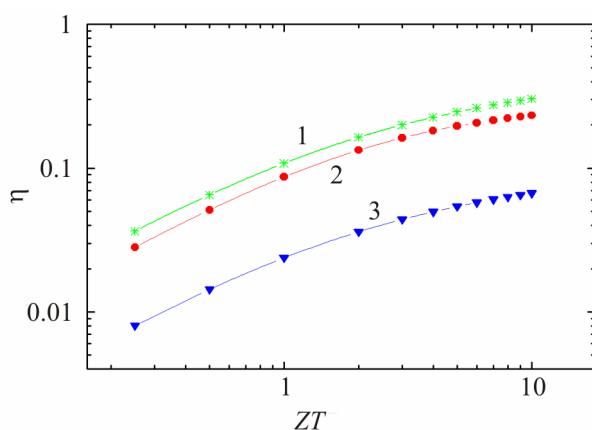


Fig. 6. The efficiency η^{ATEG} versus thermoelectric figure of merit ZT of thermocouple leg materials. Modes: 1 – maximum efficiency; 2, 3 – maximum power. Theories: 1, 2 – Ioffe [19]; 1, 3 – Okhotin [20] ($T_h = 600$ K; $T_c = 300$ K).

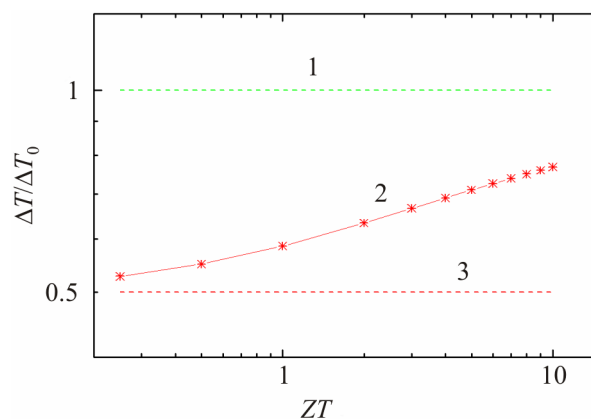


Fig. 7. The ratio of operating temperature difference ΔT on ATEG legs to temperature difference of heat-carriers $\Delta T_0 = (T_h' - T_c')$ in maximum power mode versus figure of merit ZT of materials. Theories: 1 – Ioffe [19]; 2, 3 – Okhotin [20]; 3 – Lenz's rule.

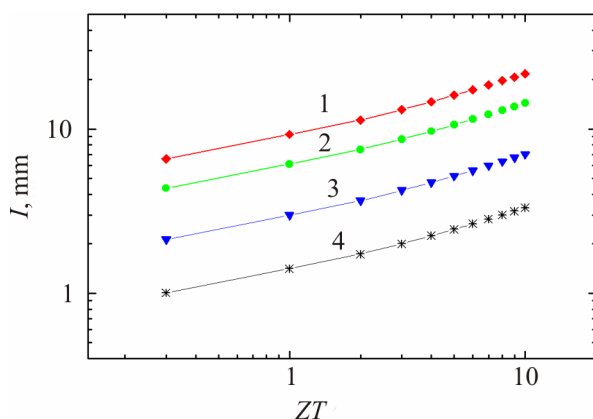


Fig. 8. The optimum length of legs l of ATEG (1 – 3) and TEG versus thermoelectric figure of merit ZT (water cooling). Leg materials: 1 – PbTe; 2, 4 – Bi_2Te_3 ; 3 – “phonon glasses”. Thermal conductivity κ , W/(cm·K): 1 – 0.025; 2, 4 – 0.015; 3 – 0.005. Theories: 4 – Ioffe [19]; 1 – 3 – Okhotin [20].

2.4. The Lenz rule

According to Lenz's rule for electric circuits, maximum power W_e of ATEG as electric engine is achieved with equal electrical resistivities of legs (r) and the load (R) ($r = R$) (Fig. 9 b) [19, 20]. On the other hand, according to Lenz's rule for thermal circuits, the maximum thermal head ($Q\Delta T$) on ATEG legs is achieved with equal thermal resistances of heat exchangers and legs ($R_{TO}^T = r^T$, Fig. 9 c; $R_{TO}^T = R_2^T + R_4^T$, $r^T = R_3^T$, Fig. 4). Both theories [19, 20] apply Lenz's rule to electric circuits of ATEG (Fig. 9 b), however, it is only the Okhotin theory [20] that additionally applies Lenz's rule to its thermal circuits (Fig. 9 c) (Table 3). In the Ioffe theory [19] the thermal resistances of heat exchangers are neglected ($R_{HE}^T = 0$, Table 3), so, Lenz's rule is not applied to ATEG thermal circuits. As a result, the temperature difference on the legs turns out to be equal to available temperature difference assigned by the heat source ($\Delta T_0 = \Delta T_r$, Fig. 9 c). This approximation is well satisfied in the case of the TEGs using solid or liquid heat carriers (Table 2).

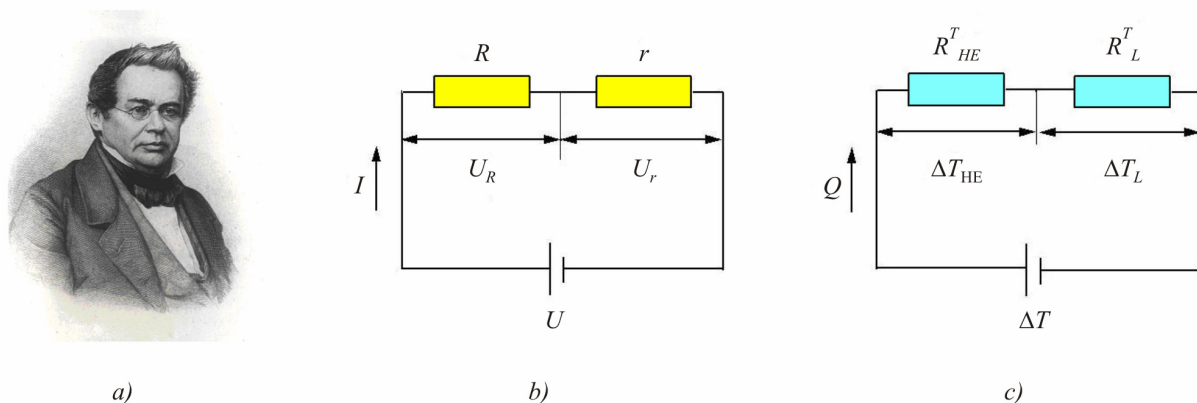


Fig. 9. Academician E.H. Lenz (1804 – 1865) (official portrait at RAS) [27, 28] (a), and application of his rule to electric ($R = r$) (b) and thermal ($R_{TO}^T = r^T$) (c) ATEG circuits.

Here: R and r are electric resistances of external load and the legs;
 R_{HE}^T and R_L^T are thermal resistances of heat exchangers and ATEG legs.

In the Okhotin theory [20], where $R_{HE}^T \neq 0$ (Fig. 9 c), the application of Lenz's rule to ATEG thermal circuits yields $\Delta T = \frac{1}{2} \Delta T_0$ for idling mode (3, Figure 7) [20].⁶ According to the theory [20], in maximum power mode the value of ΔT on ATEG legs further increases with a rise in ZT (curve 2, Figure 7) [20]. Accordingly, in the theory [20], the optimal length l of ATEG legs increases as compared to the Ioffe theory [19], but the increase in l appears proportional to the thermal conductivity κ of the TEM (curves 4 \rightarrow 1, Figure 8).

Theories [19] and [20] also give a different prediction for the value of the net power W_e of ATEG in a car (Fig. 10). Fig. 10 shows the input thermal fluxes Q_0^{ICE} , Q_0^{EP} and Q_0^{CS} in a car (a, I \rightarrow III), their share which can be taken away to ATEG (Q_0^{ATEG}) (b), and calculated net power $W_e = \eta^{ATEG} Q_0^{ATEG}$ ($\eta^{ATEG} = 0.05$) with ATEG operated in maximum power mode without account of thermal resistances of heat exchangers (the Ioffe theory [19]) (c) and with account of their contribution (the Okhotin theory [20]) (d). Fig. 10 shows that the Ioffe theory gives 3 fold overestimated values of ATEG power $W_e = 0.5; 0.17$ and 0.003 kW corresponding to placing ATEG on the internal combustion engine (I), on the exhaust pipe (II) and cooling system (III) (c). Actually, with account of parasitic thermal resistance of heat exchangers $R_{TO}^T \approx R_2^T$ we have $W_e < 0.5; 0.17$ and 0.003 kW (d, Fig.10), which is $\sim 0.5, 0.2,$ and 0.03 % of the power released at fuel combustion Q_0 (d, Fig. 10).

⁶ Earlier, Lenz's rule for ATEG thermal circuits was taken into account in [9, 24].

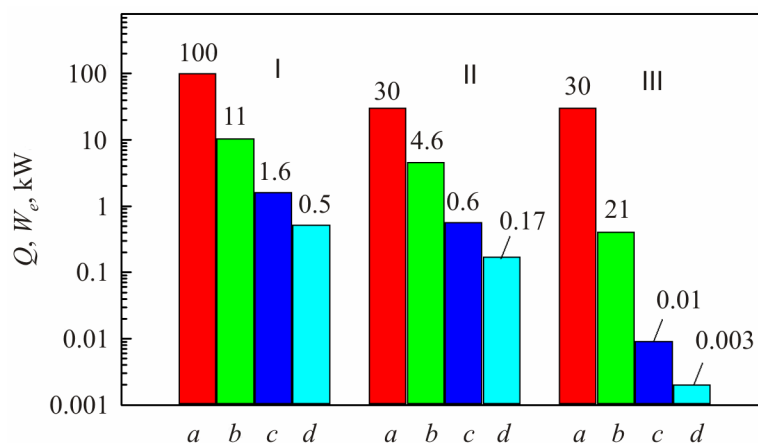


Fig. 10. Available input heat fluxes of a car Q_0 (a), their share that can be taken away to ATEG (Q_0^{ATEG}) (b), and maximum net power W_e of ATEG (c, d) (water cooling). Theories: c – Ioffe [11]; d – Okhotin [12]. ATEG location: I – ICE; II – EP; III – CS ($Q_0 = 100$ kW, $ZT = 1$).

The last estimates are in agreement with the experiment (Table 1), so the Okhotin theory [20] is a better approximation for ATEG calculations than the Ioffe theory.⁷ Further development of ATEG theory supposes a detailed account of the interaction between heat engines of "CAR-ATEG" system.

3. Conflict between ICE and ATEG

3.1. Placing ATEG in a car

A conflict between various heat engines forming one thermodynamic system is a widespread technical problem [2]. The specific feature of the conflict between ICE and ATEG in "CAR+ATEG" system is its dependence on ATEG location in a car [13]. According to Figs. 3 and 10, as a heat source for ATEG, the exhaust pipe ($Q_0^{ATEG} \leq 0.3Q_0$) and ICE ($Q_0^{ATEG} \leq Q_0$) are suitable due to appropriate parameters of R_T and $(Q_0\Delta T)$. Placing ATEG on cooling system ($Q_0^{ATEG} \leq 0.3Q_0$) is ineffective because of the smallness of R^T and $(Q_0^{CS}\Delta T)$.⁸ However, placing ATEG on ICE is not efficient either because of the conflict between ICE and ATEG that develops with increasing W_e in "CAR + ATEG" system [13-15]. Indeed, at placing ATEG in ICE, the heat engines compete for burnt fuel power Q_0 [15]. In this case the conflict between heat engines evolves rapidly with increase in W_e resulting in a sharp decrease in the overall efficiency of (ICE + ATEG) system

$$\eta^{ICE+ATEG} = \eta^{ICE} (1 - \delta) + \eta^{ATEG} \delta, \quad (3)$$

where $\delta = Q_0^{ATEG}/Q_0$ is the share of heat rejected from internal combustion engine to ATEG [15]. The reduction of $\eta^{ICE+ATEG}$ has a simple physical meaning because part of burnt fuel power Q_0 is used by less efficient heat engine ($\eta^{ATEG} \ll \eta^{ICE}$) [2, 15]. For this reason, ATEG is not currently installed in ICE, despite the large available thermal head $(Q\Delta T)$ and the acceptable value of thermal resistance R_T^{ICE} (1, Figure 5) [17, 18].⁹

On the other hand, at placing ATEG on exhaust pipe, both heat engines compete for peripheral

⁷ The Ioffe theory [19] was used for ATEG calculation in [1, 3-6], owing to which the expected characteristics proved to be overestimated (Table 1).

⁸ According to our estimate, the efficiency of cooling system waste heat recovery can be increased by a factor of 10 and more by placing the hot junctions of ATEG thermocouples in the internal combustion engine case.

⁹ Placing ATEG in the internal combustion engine may prove to be efficient in the future on achievement of $\eta^{ATEG} - \eta^{ICE}$ parity as a result of increase in TEM ZT .

thermal fluxes in the system (Q_0^{EP} and Q_0^{CS}), and the conflict between heat engines is reduced accordingly. In this case, the basic influence of ATEG on the work of internal combustion engine is expressed in the reduction of exhaust pipe temperature (T^{EP}) and in the rise of cooling system temperature (T^{CS}) [13]. Note that the Ioffe theory [19] does not predict any reduction of T^{EP} temperature (Table 3), whereas in the theory of Okhotin [20] a reduction of T^{EP} temperature for high-power ATEG may prove to be considerable (up to 100K) [13]. As a result, the value W_e of ATEG is limited at the expense of decrease in the Carnot factor η_C and owing to coke deposition on the internal side of exhaust pipe which makes heat exchange difficult (4, Fig. 4) [13, 14]. According to our estimate, with coke layer thickness $d = 0.3$ mm, the value W_e of ATEG can decrease by a factor of 3 to 5 [17-18]. On the other hand, increase in T^{EP} results in the overload of cooling system which necessitates power increase of cooling system drives ($\Delta W_C^{AT\Theta\Gamma}$) [13-15]. Assuming for simplicity that $\Delta W^{CS} \sim 0.03 Q_1^{ATEG}$, where Q_1^{ATEG} is output heat flux power of ATEG, we get $\Delta W_C^{ATEG} \sim W_e$. Thus, with regard to ΔW_C^{ATEG} the real power of waste heat recovery ΔW can essentially decrease as compared to account of only mass-factor m^* of ATEG (Table. 1) [18].

3.2. Real operating modes of ATEG

Fig. 11 shows a reduction in automotive waste heat recovery power ΔW (1) with a rise in ATEG W_e with consecutive account of the contribution of ATEG mass-factor m^* ($1 \rightarrow 2$), as well as additional power expenses for ATEG cooling ΔW_C^{ATEG} ($2 \rightarrow 3$). In the calculation of ATEG m^* (Fig. 11) it was assumed that $m^{ATEG} = k_m \cdot m_L$, where m_L is overall mass of leg materials (Bi_2Te_3) (2), $k_m = 2$ is the factor that takes into account the mass of ATEG armature. From Fig. 11 it is evident that with account of losses due to ATEG mass-factor m^* , the system passes from a mode of ideal waste heat recovery (A) ($\Delta W = W_e$) into a mode of real waste heat recovery (B), where fuel saving is still possible, ($0 < \Delta W < W_e$, $\delta A < 0$). Then, with additional account of service expenses ΔW_C^{ATEG} (4), the system passes into simple energy generation mode (C), where fuel consumption by a car is increased ($\Delta W < 0$, $\delta A > 0$) (Fig. 11) [17, 18].

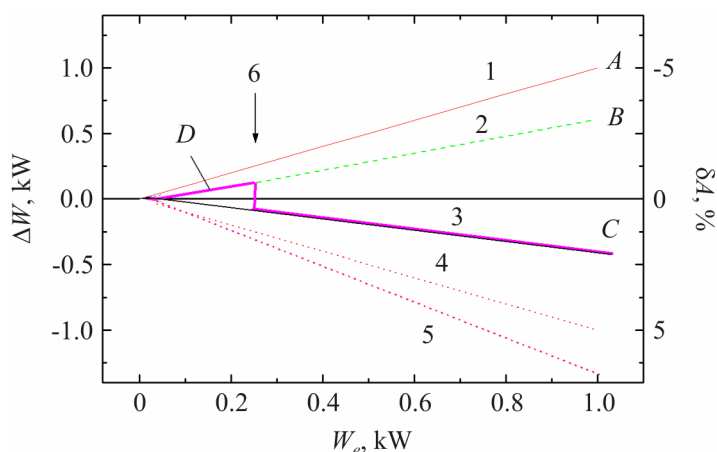


Fig. 11. Waste heat recovery ΔW of a car versus ATEG power (1–3). Modes: 1 –without regard to losses ($\Delta W = W_e$); 2 – account of losses due to motion; 3 – account of losses due to cooling system (CS) cooling and motion (5). Losses: 4 – due to CS cooling; 5 – CS cooling and motion; Modes: A – ideal waste heat recovery; B, D – real waste heat recovery; C – simple generation of energy; D – the use of CS reserves. 6 – the moment of switching additional power of CS drives. (CS reserve – 30 % (9 kW), $Q_0 = 100$ kW; $k_m = 2$; $\eta^{ATEG} = 0.03$; $l = 6$ mm; Bi_2Te_3).

From Fig. 11 follows that at small net powers $W_e \geq 0$ and $\Delta W_C^{\text{ATEG}} = 0$ (interval D) any ATEG can work in a car in a mode of real waste heat recovery (B) at $\Delta W_C^{\text{ATEG}} = 0$, provided the reserves of standard automotive cooling system are used for cooling cold junctions of ATEG [14]. Extent of interval D in Fig. 11 corresponds to cooling system reserve of cooling power $\Delta W_C \sim 30\%$ (9 kW). When a larger power comes from ATEG to cooling system (at $W_e > 0.2$ kW), additional cooling systems drives are switched on (arrow 6, Fig. 11) and ATEG passes into simple energy generation mode (C), where fuel consumption of a car is increased ($\Delta W < 0$, $\delta A > 0$). Thus, using a combined operation mode DC (Fig. 11), one can, if necessary, either reduce W_e to increase waste heat recovery power ΔW , or, on the contrary, increase W_e , converting ATEG into simple energy generation mode.

Fig. 12 shows dependences of ATEG effective efficiency $\eta_e^* = \eta^{\text{AUTO}}(W_e/\Delta W_R^*)$ versus W_e in the described B , C and D modes (Fig. 11). From Fig. 12 it is evident that in a mode of real waste heat recovery (B and D) the value η^* of ATEG appears enough high (~ 0.5) (B).

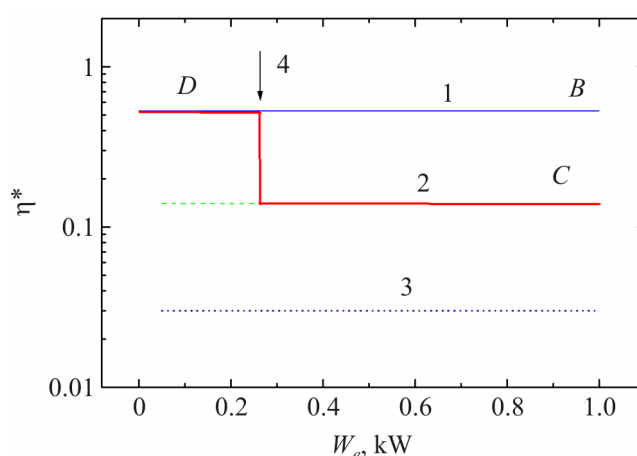


Fig. 12. Dependences of effective efficiency $\eta^ = \eta^{\text{AUTO}}W_e/\Delta W^{\text{ACE}}$ of electric energy generation by means of ATEG in a car. Modes: B , D – real waste heat recover (1); C – simple generation of energy (2); 3 – individual efficiency of ATEG as a heat engine; 4 – the moment of switching additional power of cooling system drives.*

In going to simple energy generation mode (C) the value η^* decreases to ~ 0.12 , but also essentially exceeds own efficiency of ATEG as heat engine ($\eta^{\text{ATEG}} \sim 0.03$) (3, Fig. 12). The mechanism of increase in effective efficiency $\eta^{\text{ATEG}*}$ in a car in B , C and D modes (Fig. 11) has a simple physical meaning [18]. As it is known, ATEG uses automotive waste heat which does not demand fuel consumption increase (δA) per se [1]. The fuel consumption increase ($\delta A > 0$) is necessary only for indemnification of service expenses of ICE for transportation ($\Delta W_T > 0$) and cooling of ATEG cold junctions ($\Delta W_C^{\text{ATEG}} \geq 0$). These indemnifications are made at the expense of power increase of ICE which is heat engine with higher efficiency than ATEG ($\eta^{\text{ICE}} = 0.2 - 0.4$). Thus, the ratio $\eta^{\text{ATEG}*} > \eta^{\text{ATEG}}$ (1 – 3, Fig. 12) is a consequence of co-operative effect in “CAR + ATEG” system [18]. The above described power saving operation modes of ATEG (B , C , D , Fig. 11 and 12) are of practical interest. Thus, in all the modes (B , C , D , Fig. 11 and 12) the overall performance of ATEG can be raised at the expense of using new TEM with improved characteristics [13, 14].

4. Thermoelectric materials for ATEG

Fig. 13 shows the temperature dependences of dimensionless figure of merit ZT and the optimum band gap $E_g^{\text{opt}} \sim 8k_0T$ (here k_0 is the Boltzmann constant) of TEM suitable for ATEG. The

available temperature differences ΔT_0 for gasoline and diesel engines (*b, d*) and their real values (*a, c*), reduced because of thermal resistance of heat exchangers are shown.

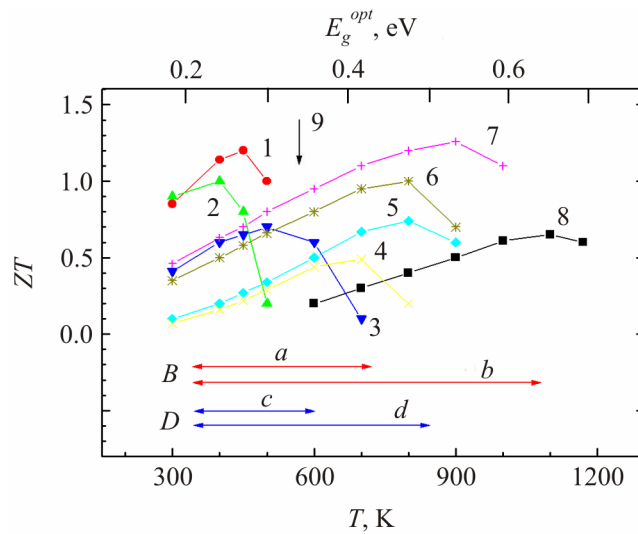


Fig. 13. The temperature dependences of dimensionless figure of merit ZT and optimum band gap E_g^{opt} of thermoelectric materials. 1 – $n\text{-Bi}_2\text{Te}_{2.7}\text{Se}_{0.3} <I, In>$ [29]; 2, 3 – $\text{Bi}_2\text{Te}_3 - \text{Sb}_2\text{Te}_3$ [30, 31]; 4 – $p\text{-Mg}_2\text{Si}_{0.4}\text{Sn}_{0.6}$ [23]; 5 – PbTe [31]; 6 – $n\text{-Mg}_2\text{Si}_{0.4}\text{Sn}_{0.6}$ [32]; 7 – $\text{AgPb}_x(\text{SbTe})_{1-x}$ (LAST) [31]; 8 – Ge-Si [31]; 9 – “dip”. Temperature differences on ATEG legs ΔT : *b, d* – available; *a, c* – real. The engines: *a, b* – gasoline; *c, d* – diesel.

From Fig. 13 it is evident that theories of Ioffe [19] and Okhotin [20] give essentially different criteria of searching for new thermoelectric materials for ATEGs. According to the Ioffe theory [19], for ATEG one needs materials with the energy gap $E_g^{opt} = 0.4 - 0.6$ eV ($T_{max} = 700 - 1100$ K) (*d, b*, Fig. 13). From [30, 31] it follows that exactly TEM with $E_g^{opt} = 0.4 - 0.6$ eV have been intensively developed by some specialists recently (5, 7, Fig. 13). However, with account of Lenz’s thermal rule (Fig. 9), the real temperature differences ΔT on ATEG legs will be lower – $E_g^{opt} \sim 0.25 - 0.4$ eV ($T_{max} = 400 - 700$ K) (*a, c*, Fig. 13) [20]. Such alloys with $E_g^{opt} \sim 0.25 - 0.4$ eV are not available now which is indicated by a “dip” in the range of temperatures $T = 400 - 700$ K existing on the family of curves $ZT = f(T)$ (marked by arrow 9, Fig. 13). From the TEM now available, the best fit for ATEG is given by alloys of the type Bi-Sb-Te-Se with $E_g \sim 0.2$ eV (2, Fig. 9) which are widely used by ATEG developers (Table 1). Recently, we have managed to increase maximum ZT of these alloys and shift it a little towards high temperatures by doping with In (1, Fig. 13) [29]. Among other materials suitable for ATEG, one can mention alloys based on Mg-Si-Sn with a low density $d \sim 3$ g/cm³ and energy gap $E_g = 0.5$ eV slightly above the optimum (6, 7, Fig. 13). The use of alloys based on Mg-Si-Sn can lead to essential decrease in the mass-factor m^* of ATEG [23, 32].

5. Discussion

Technology of automotive waste heat recovery using ATEG has been developed since the mid XX century in different countries [12]. However, an efficient ATEG has not been created to this day, which is generally attributable by ATEG developers to technical difficulties [1, 3-7]. The specified term (over 50 years) essentially exceeds the usual time for development of any technical product (several years). It shows that not only technical problems prevent from successful solution of ATEG problem [13-14].

In the present work it is established that automotive waste heat recovery using ATEG has rigid thermodynamic restrictions. This conclusion is based on the analysis of the results of experimental research on serial ATEG prototypes developed recently for motorcycles, cars and trucks [1, 3-7]. It is shown that in all the cases the experimental characteristics of ATEG appear to be essentially lower than the calculated ones [1, 3-7]. In this work, it is attributable to use in calculations of the Ioffe theory [19] that does not take into consideration high thermal resistance of heat exchangers on the “exhaust gas/exhaust pipe” boundary. As a result, the expected characteristics of ATEG have proved to be overestimated, and the prospects for using ATEG in cars overoptimistic [1, 3-7].

On the other hand, low experimental characteristics obtained in practice for modern ATEGs (Table 1) have been explained in the work by means of the Okhotin theory [20] that takes into account consistently high parasitic thermal resistance of ATEG heat exchangers on the “exhaust gas/exhaust pipe” boundary [2]. An additional factor reducing characteristics of ATEG is heterogeneity of ATEG and internal combustion engine as heat engines causing heat exchange difficulties in “CAR + ATEG” system. Besides, with a rise in W_e , a conflict of heat engines (internal combustion engine and ATEG) is developed in “CAR + ATEG” system, limiting growth of ATEG W_e and ΔW . As consequence, specific power of ATEG \dot{W}^{ATEG} is essentially inferior to that of other TEG types using liquid or solid heat-carriers (Table 2) [18].

Accordingly, the basic way for ATEG performance enhancement seems to be perfection of their heat exchangers (a reserve in specific power \dot{W}^{ATEG} up to 10 times and more) [18]. In this case, the increase in ZT of TEM, by our estimates, can be only of auxiliary nature now (a real reserve in \dot{W}^{ATEG} up to 2 times). This conclusion is proved by the literary data. Really, the greatest progress in ATEG performance enhancement has been achieved recently by improvement of ATEG heat exchangers design [3, 9, 11, and 26]. It would seem that now, alongside with perfection of heat exchangers, one should not rule out the use of power saving ATEG operation modes described in the present work (Fig. 11 and 12). Examples of using similar ATEG operation modes by the manufacturers can be found in the literature. It is demonstration of the efficiency of automotive waste heat recovery by an example of low-power ATEG ($W_e \leq 0.2$ kW) [6]. There were also proposals of replacement (full, or partial) of belt-driven automobile generators by more advanced ATEGs with increased efficiency $\eta^{\text{ATEG}*} > 0.1 - 0.5$ [10].

Conclusions

1. Installation of automotive thermoelectric generator (ATEG) on a car exhaust pipe creates essential thermodynamic restrictions on the value of generated net electric power W_e and recovered energy ΔW .
2. Therefore, the prospects of using high-power ATEGs for waste heat recovery and fuel consumption decrease in automobiles ($\Delta W > 0$, $\delta A < 0$) are essentially limited now.
3. Nevertheless, ATEGs of moderate power can be efficiently used in automobiles in waste heat recovery and simple energy generation modes, with regard to their high net efficiency ($\eta^{\text{ATEG}*} > 0.1 - 0.5$), increased due to cooperative effect in “CAR + ATEG” system.

References

1. C.B. Vining, The Limited Role for Thermoelectrics in Climate Crisis, *J. Thermoelectricity* **4**, 7-19 (2008).
2. V.A. Kirillin, V.V. Sychev, A.V. Sheindlin, *Technical Thermodynamics* (Moscow: Energiya, 1974), 448 p.

3. K.M. Saqr, M.K. Mansour, and M.N. Musa, Thermal Design of Automobile Exhaust-based Thermoelectric Generators: Objectivities and Challenges, *International J. Automotive Technology* 9(2), 155- 160 (2008).
4. D.M. Rowe, J. Smith, G. Thomas and G. Min, Weight Penalty Incurred in Thermoelectric Recovery of Automobile Exhaust Heat, *J. Electronic Materials* 40 (5), 784-788 (2011).
5. J. Lieb, S. Neugebauer, A. Eger, M. Linde, B. Masar, W. Stütz, The Thermoelectric Generator from BMW is Making Use of Waste Heat, *MTZ* 70 (4) 4-11 (2009).
6. A. Eger, M. Linde, *The BMW Group. Roadmap for the Application of Thermoelectric Generators* (San Diego, 2011), 23 p.
7. T. Kajikawa, Advances Thermoelectric Power Generation in Japan, *J. Thermoelectricity* 3, 5-18 (2011).
8. N. Espinosa, M. Lazard, L. Aixala, and H. Scherrer, Modeling Thermoelectric Generator Applied to Diesel Automotive Heat Recovery, *JEMS* 39(9), 1446-1455 (2010).
9. L.I. Anatychuk, O.J. Luste, and R.V. Kuz, Theoretical and Experimental Study of Thermoelectric Generators for Vehicles, *JEMS* 40 (5), 1326-1331 (2011).
10. J.W. Fairbanks, Development of Automotive Thermoelectric Generators and Air Conditioner / Heaters, *Proceedings of XIV International Forum on Thermoelectricity* (Moscow 17-20.05.2011), [On line: <http://forum.inst.cv.ua/>].
11. L.I. Anatychuk, R.V. Kuz, and Yu.Yu. Rozver, Thermoelectric Generators for Gasoline Engines, *J. Thermoelectricity* 2, 81-94 (2012).
12. E.M. Fajnzilber, L.M. Drabkin, Use of Heat of the Fulfilled Gases of Engines in the Thermoelectric Generator for a Power Source of Elements of an Electric Equipment of Cars, *Automotive Industry* 7, 9-10 (1996).
13. M.A. Korzhuev, Yu.V. Granatkina, Some Bottlenecks in the Automobile Thermoelectric Generators and a Search for New Materials to Eliminate Them, *J. Thermoelectricity* 1, 81-94 (2012).
14. M.A. Korzhuev, Conflict between Internal Combustion Engine and Thermoelectric Generator during Waste Heat Recovery in Cars, *Technical Physics Letters* 37 (4), 8-15 (2011).
15. M.A. Korzhuev, I.V. Katin, On the Placement of Thermoelectric Generators in Automobiles, *JEMS* 39 (9), 1390-1394 (2010).
16. M.A. Korzhuev, I.V. Katin, Reduced Life Time of the Vehicles by Installation of Thermoelectric Generator on Exhaust Pipe of the Internal Combustion Engine, *Chaos and Structures in Nonlinear Systems. Theory and Experiment* (Karaganda: E.A. Buketov State University, 2012), p. 250-254.
17. M.A. Korzhuev, I.V. Katin, Potential Economic Impacts of the Thermoelectric and Automobile Industries Associated with the Start of Mass Production of Automotive Thermoelectric Generators, *Thermoelectrics and their Applications*. Ed. by M.I. Fedorov and L.N. Lukyanova [On line:] <http://www.ioffe.ru/Thermolab>
18. M.A. Korzhuev, I.V. Katin, Some Features of Automotive Thermoelectric Generators (ATEG) and the Prospects for their Use in Transport, *Thermoelectrics and their Applications*. Ed. by M.I. Fedorov and L.N. Lukyanova [On line:] <http://www.ioffe.ru/Thermolab>
19. A.F. Ioffe, *Semiconductor Thermoelements* (Moscow-Leningrad: USSR Acad.Sci., 1960).
20. A.S. Okhotin, A.A. Efremov, V.S. Okhotin, and A.S. Pushkarsky, *Thermoelectric Generators* (Moscow: Atomizdat, 1976), 320 p.
21. B.S. Pozdnyakov, E.A. Koptelov, *Thermoelectric Power* (Moscow: Atomizdat, 1974), 264 p.
22. G.K. Kotyrlo, Yu.N. Lobunets, *Calculation and Designing of Thermoelectric Generators and Thermal Pumps. Handbook* (Kyiv: Naukova Dumka, 1980).
23. Yu.G. Manasian, *Ship's Thermoelectric Devices and Installations* (Leningrad: Sudostroyeniye,

- 1968), 284 p.
24. G.J. Snyder, Thermoelectric Power Generators. Efficiency and Compatibility, In: *Thermoelectric Handbook. Macro to Nano*. Ed: D.M. Rowe (CRC Press. Taylor & Francis.: Boca Raton, London, N.Y., 2006), P. 9.1-9.26.
 25. L.I. Anatychuk, *Thermoelectricity. V. 2. Thermoelectric power converters* (Kyiv, Chernivtsi: Institute of Thermoelectricity, 2003), 376 p.
 26. S.N. Plehanov, V.E. Novikov, and A.J. Terekov, Thermoelectricity in Russia – 250 years, *Thermoelectrics and their Applications*. Ed. by M.I. Fedorov and L.N. Lukyanova [On line:] <http://www.ioffe.ru/Thermolab>
 27. *Academy of Sciences of the USSR. Personal structure (1724-1917). Book 1* (Moscow: Science, 1974), 480 p.
 28. M. Gliozzi, *Storia della fisica* (Torino, Italy, 1965), 464 p.
 29. T.E. Svechnikova, I.Yu. Nikhezina, M.A. Korzhuev, Thermoelectric Properties of $n\text{-Bi}_2\text{Te}_{2.7}\text{Se}_{0.3}\langle\text{I, In}\rangle$ Crystals, *Inorganic Materials* **47**(12), 1314-1318 (2011).
 30. G.S. Nolas, J. Sharp, H.J. Goldsmid, *Thermoelectrics. Basic Principles and New Materials Developments* (Springer, Berlin, Heidelberg, N.Y, 2001).
 31. J.R. Sootsman, D.Y. Chung, and M.G. Kanatzidis, New and Old Concepts in Thermoelectric Materials, *Angew. Chem. Int. Ed.* **48**, 8616-8639 (2009).
 32. G.N. Isachenko, V.K. Zaitsev, M.I. Fedorov, T.A. Gurieva, and P.P. Konstantinov, Thermodynamic Properties of Solid Solutions between p -type Compounds Mg_2X ($\text{X} = \text{Si}, \text{Ge}, \text{Sn}$), *Thermoelectrics and their Applications*. Ed. by M.V. Vedernikov and L.N. Lukyanova (SPb: PIYF, 2010), P. 99-102.

Submitted 01.03.2013.